Journal of Assisted Reproduction and Genetics
https://doi.org/10.1007/s10815-020-02005-z

REPRODUCTIVE PHYSIOLOGY AND DISEASE

Adipose tissue–derived stem cells protect the primordial follicle pool from both direct follicle death and abnormal activation after ovarian tissue transplantation

Luciana Cacciottola[1] · Guillaume E. Courtoy[2] · Thu Y. T. Nguyen[1] · Camille Hossay[1] · Jacques Donnez[3] · Marie-Madeleine Dolmans[1,4]

Received: 11 September 2020 / Accepted: 3 November 2020
© Springer Science+Business Media, LLC, part of Springer Nature 2020

Abstract

Purpose To investigate whether adipose tissue–derived stem cells (ASCs) protect the primordial follicle pool, not only by decreasing direct follicle loss but also by modulating follicle activation pathways.

Methods Twenty nude mice were grafted with frozen-thawed human ovarian tissue from 5 patients. Ten mice underwent standard ovarian tissue transplantation (OT group), while the remaining ten were transplanted with ASCs and ovarian tissue (2-step/ASCs+OT group). Ovarian grafts were retrieved on days 3 ($n = 5$) and 10 ($n = 5$). Analyses included histology (follicle count and classification), immunohistochemistry (c-caspase-3 for apoptosis and LC3B for autophagy), and immunofluorescence (FOXO1 for PI3K/Akt activation and YAP for Hippo pathway disruption). Subcellular localization was determined in primordial follicles on high-resolution images using structured illumination microscopy.

Results The ASCs+OT group showed significantly higher follicle density than the OT group ($p = 0.01$). Significantly increased follicle atresia ($p < 0.001$) and apoptosis ($p = 0.001$) were observed only in the OT group. In primordial follicles, there was a significant shift in FOXO1 to a cytoplasmic localization in the OT group on days 3 ($p = 0.01$) and 10 ($p = 0.03$), indicating follicle activation, while the ASCs+OT group and non-grafted controls maintained nuclear localization, indicating quiescence. Hippo pathway disruption was encountered in primordial follicles irrespective of transplantation, with nuclear YAP localized in their granulosa cells.

Conclusion We demonstrate that ASCs exert positive effects on the ovarian reserve, not only by protecting primordial follicles from direct death but also by maintaining their quiescence through modulation of the PI3K/Akt pathway.

Keywords Ovarian tissue transplantation · Adipose tissue–derived stem cells · Primordial follicles · Follicle activation · PI3K/Akt pathway

Introduction

As infertility after gonadoxic treatment is becoming a major concern in young cancer survivors, oncofertility counseling to discuss fertility preservation options has gained increased awareness over recent years [1]. Among available options, ovarian tissue cryopreservation followed by transplantation is a valid and effective technique and the only alternative for prepubertal patients and women who cannot delay their oncological treatments [2]. Although more than 200 live births have been reported, with an exponential increase in the last few years [3], there are still numerous issues arising from the avascular nature of the grafting procedure itself [4]. Transplanted ovarian cortex fragments undergo a period of hypoxia lasting 5–10 days before their revascularization is

✉ Marie-Madeleine Dolmans
marie-madeleine.dolmans@uclouvain.be

1 Gynecology Research Unit, Institut de Recherche Expérimentale et Clinique, Université Catholique de Louvain, Av. Mounier 52, bte B1.52.02, 1200 Brussels, Belgium

2 IREC Imaging Platform, Institut de Recherche Expérimentale et Clinique, Université Catholique de Louvain, Av. Hippocrate 55, 1200 Brussels, Belgium

3 Society for Research into Fertility, Av. Grandchamp 143, 1150 Brussels, Belgium

4 Department of Gynecology, Cliniques Universitaires Saint-Luc, Av. Hippocrate 10, 1200 Brussels, Belgium

Published online: 12 November 2020

complete [5]. Moreover, during this progressive revascularization, oxidative stress levels rise and persist much longer, until complete reestablishment of the tissue and its metabolism [6]. As a consequence of exposure to ischemic and oxidative stress damage, the ovarian follicle pool suffers massive follicle death, loosing between 50 and 90% of follicles [6, 7]. In recent years, another possible cause of massive follicle depletion has been suggested, namely a response to tissue damage. Indeed, a number of authors investigated the possibility of massive activation and evolution of primordial follicles to growing stages due to dysregulation of follicle recruitment mechanisms. This may occur in the ovary in response to tissue injury, acting as protection against chemotherapy-related damage, but results are discrepant [8]. While some authors observed greater activation of primordial follicles after cyclophosphamide exposure [9], others found only an increase in apoptosis signaling indicative of a damage response in ovarian tissue [10].

Primordial follicle recruitment is normally regulated by highly controlled mechanisms, which maintain a balance between quiescence and growth. Among them, the phosphoinositol-3-kinase (PI3K)/protein kinase B (Akt) signaling pathway is known to be one of the major elements responsible for primordial follicle activation [11, 12]. This signaling cascade is fundamental to several cell processes, including cell survival, growth, and apoptosis. Upon Akt phosphorylation by various molecules and growth factors, a number of effectors are activated, including forkhead box 01–3 (FOXO1–3) and the mechanistic target of rapamycin complex (mTORC1). The Hippo pathway has also been identified as a major follicle growth regulator [12]. This signaling cascade is modulated by mechanical forces delivered to tissues to control organ growth, and hence may be dysregulated by mechanical manipulation of ovarian fragments [13]. It functions through its action on the yes-associated protein (YAP)/transcriptional coactivator with PDZ-binding motif (TAZ) which, once unphosphorylated, shifts to the nucleus to activate transcription factors like the TEA domain family 1–4 (TEAD1–4) [12, 13].

These activated signaling pathways were investigated in ovarian tissue after transplantation. An increase in PI3K/Akt signaling was observed early after transplantation [14], as was an important shift from quiescent to growing stages [15]. This activation may be driven by molecules and growth factors released in hypoxic conditions, like vascular endothelial growth factor (VEGF) activated by hypoxia-inducible factor-1 (HIF-1) signaling [16, 17]. Nevertheless, conclusions on the impact of follicle activation in accelerated follicle pool depletion and its relationship with hypoxia remain contentious.

We recently developed a strategy to reduce follicle loss after human ovarian tissue transplantation, which involves preparation of the grafting site with adipose tissue–derived stem cells (ASCs) embedded in fibrin scaffolds 2 weeks before transplantation [18, 19]. ASCs are known to exert proangiogenic effects by endothelial lineage differentiation and growth factor secretion [20]. In our xenotransplantation model, they proved capable of shortening hypoxia and boosting revascularization, with a significant increase in follicle survival rates [19]. ASCs not only ensure a decrease in follicle death at all stages because of a shorter hypoxic period but also exhibit different interactions with cell survival mechanisms and cell death signaling pathways soon after transplantation.

The aim of the present study was to investigate the effect of the hypoxic period occurring soon after transplantation on (i) primordial follicle activation through modulation of the PI3K/Akt and Hippo signaling pathways, and (ii) primordial follicle death by modulation of apoptosis and autophagy. Indeed, our goal was to determine whether a reduction in hypoxia after grafting with ASCs is able to positively regulate primordial follicle behavior in human transplanted tissue.

Material and methods

Experimental design

A total of 20 nude mice (Swiss nu/nu, Charles River Laboratories, France) were grafted with frozen-thawed human ovarian tissue from 5 different patients. Ovarian fragments were equally distributed between (i) 10 mice undergoing 2-step transplantation with ASCs (2-step/ASCs+OT group) and (ii) 10 mice undergoing one-step transplantation (OT group). As previous studies have shown comparable findings between one-step transplantation and the 2-step procedure using empty fibrin, the latter group was not added as an additional control [19]. The 2-step procedure involved transplantation of a fibrin scaffold loaded with 1.5×10^6 ASCs for graft site preparation 14 days prior to human ovarian cortex transplantation. In each group, the mice were euthanized for graft retrieval in a staggered fashion, on post-transplantation days 3 ($n = 5$) and 10 ($n = 5$) respectively. One tissue fragment was taken directly from each patient to serve as non-grafted controls (Fig. 1).

Ovarian tissue consent and thawing procedure

The Institutional Review Board of the Université Catholique de Louvain approved use of human ovarian tissue for this study (2012/23MAR/125). Ovarian tissue biopsies from 5 patients (age range 20–35 years) were taken from our tissue bank after obtaining written informed consent. All the women had undergone surgery for non-ovarian pathologies. Their tissue was frozen using the slow-freezing protocol, as previously described [21]. Cryogenic vials were thawed at room temperature (RT) for 2 min, immersed in a water

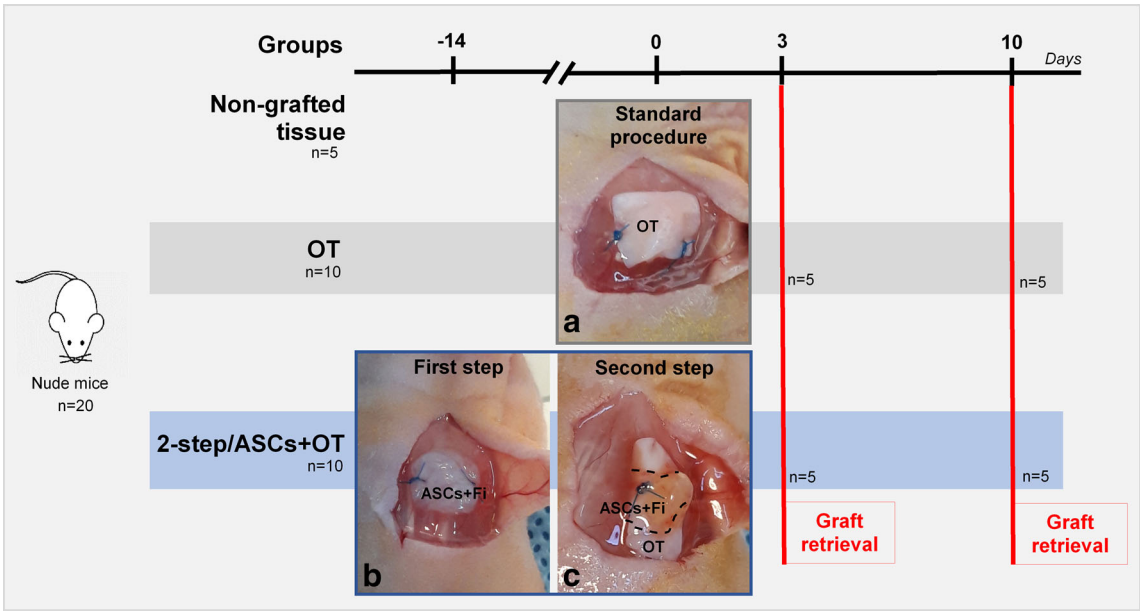


Fig. 1 Experimental design. Ovarian tissue from 5 patients was distributed equally between three groups: one piece for non-grafted controls and the other two for xenografting using either standard transplantation (OT group) (A) or 2-step transplantation, first grafting ASCs loaded inside a fibrin scaffold (B) and then performing transplantation (C) (2-step/ASCs+OT group). Mice were euthanized on days 3 and 10, and samples were collected for histological analyses. OTT, ovarian tissue transplantation; OT, ovarian tissue; ASCs, adipose tissue–derived stem cells; Fi, fibrin

bath at 37 °C for another 2 min, then washed three times in fresh HEPES-MEM (Gibco).

Surgical procedure

Animal welfare guidelines were strictly followed and the protocol was approved by the Committee on Animal Research of the Université Catholique de Louvain (2018/UCL/MD/40). Twenty female nude mice (Crl:NU-Foxn1nu, Swiss nu/nu, Charles River Laboratories, France) aged 8–15 weeks were used for this study. Anesthesia (isoflurane 3% for sleep induction and 2% for sleep maintenance) and analgesia (buprenorphine 0.1 mg/kg) were provided for every surgical procedure undertaken. The mice were kept in sterile conditions and fed ad libitum for the entire duration of the experiment, until euthanasia by cervical dislocation.

First step: preparation of the transplantation site

Human ASCs from female donors were commercially acquired with the following characteristics: flow cytometry cell surface protein profile positivity for CD29, CD44, CD73, CD90, CD105, and CD166 (> 95%), and negativity for CD34, CD14, CD31, CD45, and Lin1 (< 2%) (StemPRO human ASCs, Invitrogen, USA). They were cultured at passages 5–6 in growth medium (Complete MesenPRO RSTM medium, Invitrogen, USA) until an appropriate number of cells was reached, and then implanted inside fibrin scaffolds (Tisseel, Baxter, Belgium). Fibrin scaffolds were assembled by mixing ASCs (1.5×10^6 in 20 µl of medium), 40-µl fibrinogen solution (50 mg/ml), and 40-µl thrombin (50 IU/ml). These matrices were incubated for 45 min for optimal polymerization of fibrin prior to grafting [22].

Ten mice (2-step/ASCs+OT group) underwent grafting to their back muscle, which is known to be an optimal grafting site in the murine model for early revascularization and support of follicle growth, showing no significant difference with the peritoneal cavity [23]. Briefly, their back muscle was exposed making an L-shaped incision, and gently scratched with a scalpel. Previously assembled fibrin scaffolds were then transplanted to this back muscle and sutured with 2 cardinal stitches using 6/0 Prolene (Fig. 1B).

Second step: ovarian tissue transplantation

Fourteen days later, frozen-thawed ovarian tissue fragments each measuring 6 × 4 × 1.5 mm were transplanted in both groups: (i) in the 2-step/ASCs+OT group ($n = 10$), the remaining fibrin was partially detached very gently with blunt-tip forceps to create a pocket in the peritoneum where ovarian fragments were placed without additional stitches (Fig. 1C); (ii) in the OT group ($n = 10$), the fragments were placed on the back muscle after scratching the surface with a scalpel, and fixed with 2 cardinal stitches using 6/0 Prolene (Fig. 1A).

Sample collection

Ovarian fragments and grafted samples retrieved on days 3 and 10 were fixed in 4% formaldehyde for histology and immunolabeling.

Follicle outcomes

Follicle count and classification

Samples for histology were embedded in paraffin and serially cut into 5-µm-thick sections. Every 12th slide (60 µm) was stained with hematoxylin and eosin (H&E) (Merck, Germany), digitized using the Pannoramic P250 Flash III scanner (3DHistech, Hungary), and analyzed with CaseViewer (v2.3). Follicle density was determined in 12 random fragments per sample as the number of follicles per mm^3, calculating volume by multiplying digitized surfaces by fragment thickness. All morphologically normal follicles (defined by a visible oocyte) were taken into account. Follicle atresia was evaluated using specific morphological criteria, namely ooplasm eosinophilia, granulosa cell pyknosis, cytoplasmic contraction, and/or the presence of vacuoles [24]. Viable follicles were classified according to stage into primordial, primary, secondary, or antral, and the percentage of each stage was established for comparison between groups [25]. Primordial follicles were further classified into (a) small primordial, in which the oocyte is surrounded only by flattened granulosa cells, and (b) intermediate, in which the oocyte is surrounded by a mixture of flattened and cuboidal granulosa cells, according to Gougeon et al. [24, 26].

Follicle apoptosis

Paraffin sections were deparaffinized with Histosafe (Yvsolab SA, Belgium) and rehydrated in 2-propanol (Merck, Germany). After blocking endogenous peroxidase activity with 3% H2O2 and demasking in citrate buffer (pH 6) for 75 min at 98 °C, non-specific binding sites were blocked by incubation in normal goat serum for 30 min. Sections were first incubated overnight at 4 °C with rabbit anti-human cleaved caspase-3 (c-caspase-3) (1:100, G748A Promega) and then at RT for 1 h with EnVision rabbit horseradish peroxidase (HRP) (1:1, K4003, Dako, USA). Diaminobenzidine (DAB) (Dako, USA) was used as a chromogen. Negative controls were obtained using non-specific rabbit antibodies (10,133,249, Dako), and spleen tissue served as positive controls (Supplementary fig. 1).

Slides were digitized using the Pannoramic P250 Flash III scanner at × 20 magnification. All morphologically normal follicles were analyzed. Follicles were considered positive if more than 50% of granulosa cells or the oocyte were stained [27].

Follicle autophagy

Paraffin sections were deparaffinized with Histosafe (Yvsolab SA, Belgium) and rehydrated in 2-propanol (Merck, Germany). After blocking endogenous peroxidase activity with 3% H2O2 and demasking in citrate buffer (pH 6) for 75 min at 98 °C, non-specific binding sites were blocked by incubation in normal goat serum for 30 min. Sections were first incubated overnight at 4 °C with rabbit anti-human LC3B (1:500, 3868S, Cell Signaling, USA) and then at RT for 1 h with EnVision rabbit HRP (1:1, K4003, Dako, USA). DAB (Dako, USA) was used as a chromogen. Negative controls were obtained using non-specific rabbit antibodies (10133249, Dako), and adrenal gland tissue served as positive controls (Supplementary fig. 1).

All morphologically normal follicles were analyzed using the Leica SCN400 scanner at × 40 magnification. Quantitative analysis of morphologically normal follicles in granulosa cells was performed with Fiji v1.52 (National Institutes of Health, NIH, USA) using semi-automated macro image processing. Briefly, after manual delimitation of the granulosa layer as a region of interest (ROI), the signal was extracted by DAB color deconvolution and a fixed threshold was applied, considering values above the threshold as positive selection. In the ROI, total area, thresholded area, and the mean intensity of thresholded pixels were measured. Results were expressed as the staining index and calculated as follows: $\frac{(\text{area of threshold pixels in ROI}) \times (\text{mean intensity of threshold pixels in ROI})}{\text{area of ROI}}$ in absoulute units.

Follicle activation

Two main signaling pathways responsible for primordial follicle activation were analyzed: FOX01 translocation from the nucleus to the cytoplasm, reflecting activation of the PI3K/Akt pathway, and disruption of the Hippo pathway by transfer of YAP to the nucleus. Sections were deparaffinized with Histosafe (Yvsolab SA, Belgium) and rehydrated in 2-propanol (Merck, Germany). After blocking endogenous peroxidase activity with 3% H2O2 and demasking in citrate buffer (pH 6) for 75 min at 98 °C, non-specific binding sites were blocked by incubation in normal goat serum for 30 min at RT. Sections were first incubated overnight at 4 °C either with rabbit anti-human FOX01 (1:200, 2880, Cell Signaling, USA) or with mouse anti-human YAP (1:200, 12395S, Cell Signaling, USA), and then for 1 h with either EnVision rabbit HRP (1:1, K4003, Dako, USA) or EnVision mouse HRP (1:2, K001, Dako, USA). Unmasking was achieved using boric acid solution with 1:1000 H2O2 at 30% and tyramide chromogen for 15 min at RT (Alexa Fluor tyramide reagent, 1:200, B40953, Invitrogen), followed by a 20-min citrate buffer bath in the microwave. Cell nuclei were then stained by 10-min

incubation in Hoechst 333452 (1:1000, H3570, Invitrogen). Slides labeled for YAP were also incubated in wheat germ agglutinin (WGA) (1:500, Biotium) for 10 min to stain plasma membranes, before being mounted with HIGHDEF IHC fluoromount (Enzo, USA). Negative controls were obtained using non-specific rabbit antibodies (10133249, Dako) and non-specific mouse antibodies (10132024, Dako). Bowel tissue served as positive controls for FOXO1, and breast cancer tissue served as positive controls for YAP (Supplementary fig. 1).

Images of primordial follicles were taken using the Axio Imager Z1 microscope with structured ApoTome illumination and a 63x/1.4 oil objective with laser at 405, 488, and 564 nm for Hoechst 33342, tyramide chromogen, and WGA. Native images were analyzed with Fiji v1.52 (NIH, USA) to measure mean signal intensity in follicle nuclei and the cytoplasm. Briefly, each follicle was defined as a ROI. More specifically, the ROI was limited to the oocyte of primordial follicles for FOXO1 analysis, but targeted the granulosa cells of both primordial and growing follicles for YAP analysis. A fixed threshold was then applied to the blue channel (DAPI staining) to delineate the nucleus within the considered ROI. For YAP analysis, the red channel (WGA) served for precise delimitation of the cytoplasmic membrane of granulosa cells. Hence, the mean intensity of the green signal was measured in the cytoplasmic and nuclear compartments within the considered ROI in question. Results were expressed in a continuous dimension and calculated as: $x = \frac{\text{mean intensity (in nucleus)}}{\text{mean intensity (in nucleus and cytoplasm)}}$, with $x > 1$ indicative of nuclear signaling and $x < 1$ indicative of cytoplasmic signal localization.

Statistical analysis

Prism 8 for Windows (GraphPad software, USA) was used for statistical analysis. Follicle analyses were pooled to obtain mean values for each sample. For follicle density analysis between groups and time points, two-way analysis of variance (ANOVA) and Tukey's post hoc test were applied. For all other parameters, either one-way ANOVA or the Kruskal–Wallis test was used, depending on normality distribution, with Fisher's LSD or uncorrected Dunn's test as a post hoc test. Results were presented as mean ± SEM or mean ± SD, where appropriate. p values < 0.05 were considered statistically significant.

Results

Graft recovery rates and macroscopic assessment

All grafted tissues were retrieved from all 20 mice, having been attached to their back muscles. Histological analysis of H&E staining performed on ovarian fragments on day 3 evidenced dyshomogeneity in tissue samples. In fact, some central spots of necrosis were detected, with nearly follicles showing an eosinophilic cytoplasm and alterations to granulosa cell structure, but they never exceeded 10% of the whole tissue surface in any of the samples. By day 10, no further necrosis was observed in any of ovarian grafts.

Follicle density and classification

Follicle density and classification were evaluated in H&E-stained fragments. A total of 706 follicles were counted in non-grafted controls, 500 follicles in the 2-step/ASCs+OT group, and 343 follicles in the OT group 3 days post-transplantation. Ten days post-transplantation, 364 follicles were found in the 2-step/ASCs+OT group and 224 follicles in the OT group (Supplementary Table 1). Follicle density (no. follicles/mm^3 ± SD) was significantly lower in the OT group after 3 days (190.1 ± 217.9, $p = 0.03$) and 10 days (124.8 ± 103.8, $p = 0.01$) than in non-grafted controls (379.5 ± 322.4). In the 2-step/ASCs+OT group, no significant difference in follicle density was detected at any time point (day 3: 342.1 ± 428.6; day 10: 216.4 ± 263.4) (Fig. 2a).

Regarding follicle stages, densities of small primordial, intermediate, and growing (pooling primary and secondary) follicles were investigated. Small primordial follicle density decreased significantly in the OT group on days 3 (50.4 ± 81.7, $p = 0.04$) and 10 (48.1 ± 34.1, $p = 0.04$) compared to non-grafted controls (240.4 ± 189.1), while no significant difference was identified in the 2-step/ASCs+OT group (day 3: 146.4 ± 193.7; day 10: 106.4 ± 146) (Fig. 2a).

In terms of proportions of atretic follicles (Fig. 2d), a significant increase in atresia was detected in the OT group on days 3 (51.4 ± 27.5, $p < 0.001$) and 10 (26.4 ± 11.5, $p = 0.02$) compared to non-grafted controls (10.4 ± 5.5) (Fig. 2b-c), but no significant difference was observed in the 2-step/ASCs+OT group at any time point. Moreover, on day 10, atretic follicle proportions were significantly higher in the OT group than in the 2-step/ASCs+OT group (26.4 ± 11.5 vs 11.9 ± 5.8, $p = 0.03$).

Follicle apoptosis

A total of 1126 normal-looking follicles were analyzed for the c-caspase-3 marker: 338 from non-grafted controls, respectively 243 and 196 from the 2-step/ASCs+OT and OT groups on day 3, and respectively 190 and 201 from the 2-step/ASCs+OT and OT group on day 10. Proportions of c-caspase-3-positive follicles were significantly higher in the OT group after 3 (30.9 ± 10.5, vs $p = 0.001$) and 10 (18.03 ± 10.4, $p = 0.04$) days post-transplantation compared to non-grafted controls (3.7 ± 3.3), while no significant increase was detected in the 2-step/ASCs+OT group (day 3: 13.1 ± 11.7;

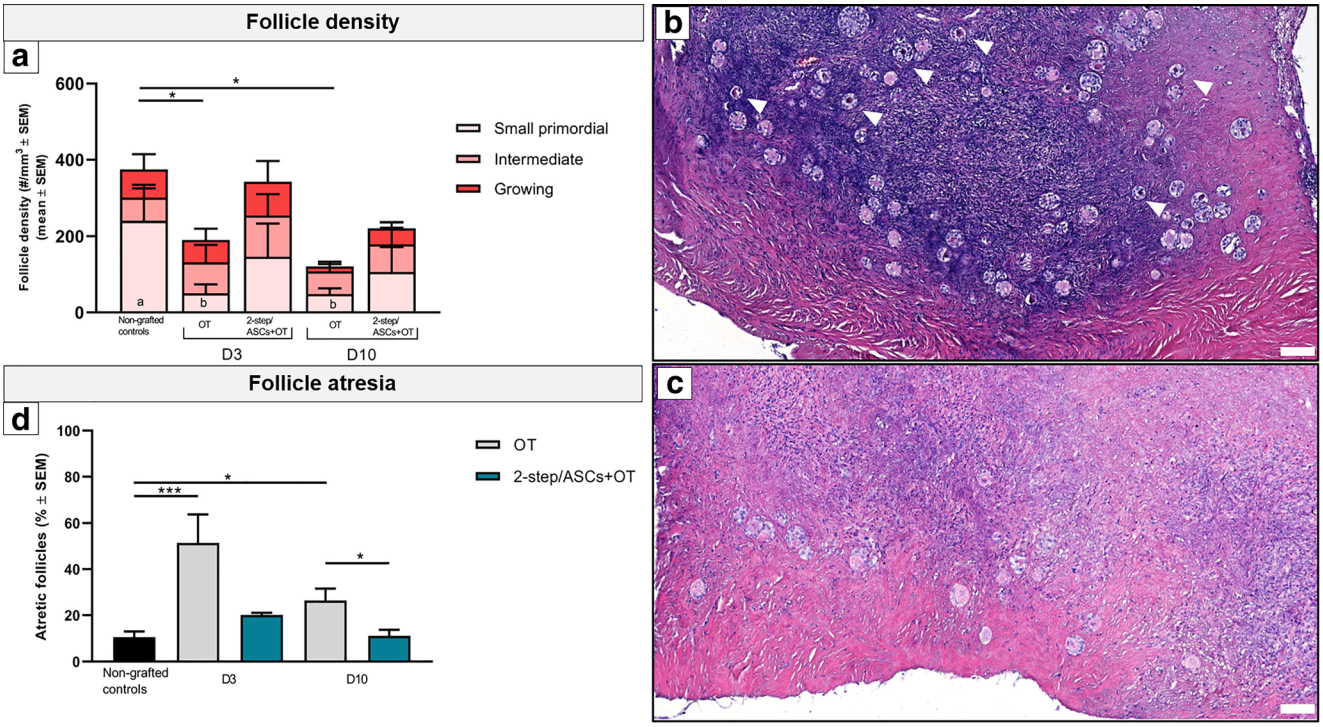


Fig. 2 Follicle outcomes. **a** Follicle density (no. of follicles/mm^3 ± SEM) in the general follicle population and at each follicle stage (small primordial, intermediate, and growing) evaluated by two-way ANOVA and Tukey's post hoc test. **b** Follicle atresia (% of atretic follicles/total follicles) evaluated by using the Kruskal–Wallis test and Fisher's post hoc test. H&E staining of grafted tissues in the OT group on day 3 (**c**) and the 2-step/ASCs+OT group on day 3 (**d**). White arrows indicate atretic follicles in the tissue. p value references: *$p < 0.05$, ***$p < 0.001$. Statistical significance is expressed in subcolumns using different letters ($p < 0.05$). Scale bar: 100 μm

day 10: 12.1 ± 6.3) (Fig. 3a). At the primordial follicle stage, significantly greater proportions of c-caspase-3-positive follicles were observed in both small primordial (non-grafted controls: 5.2 ± 1.6; OT group: 26.8 ± 4.3, $p = 0.008$) and intermediate (non-grafted controls: 2.9 ± 2.1; OT group: 32 ± 19.2, $p = 0.004$) follicles in the OT group 3 days after transplantation. Moreover, proportions of small c-caspase-3-positive primordial follicles were significantly higher in the OT group than in the 2-step/ASCs+OT group (10.4 ± 12.7, $p = 0.03$) at this time point (Fig. 3b).

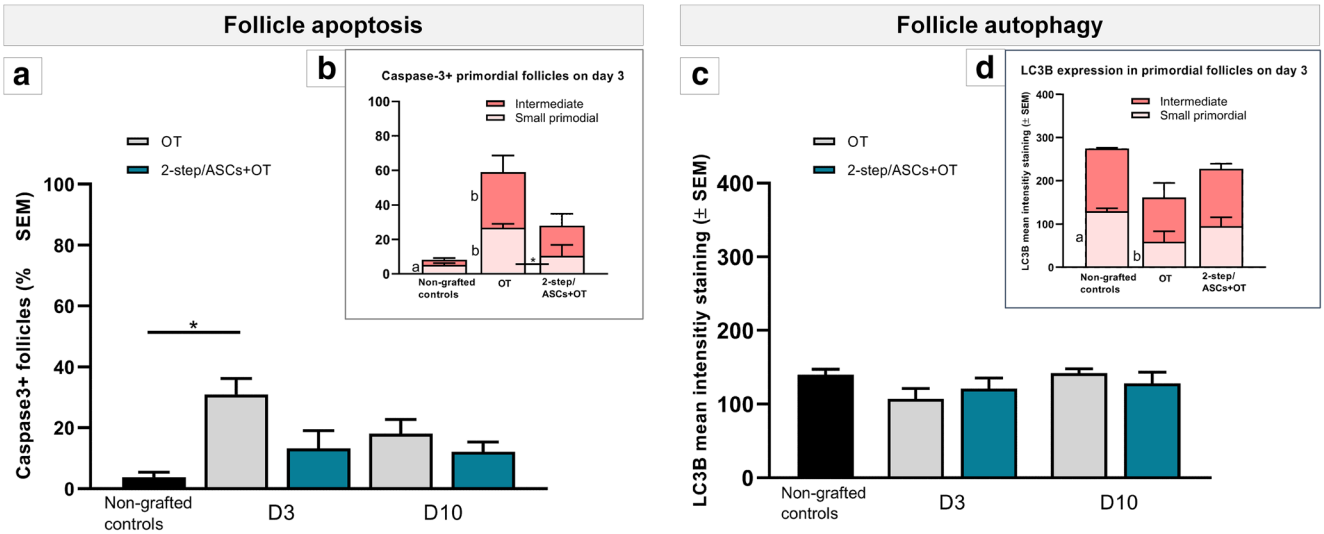


Fig. 3 Follicle apoptosis and autophagy. Follicle apoptosis (% of c-caspase-3+ follicles/total follicles ± SEM) in the general follicle population (A) and in primordial follicles on day 3 (B) evaluated by using one-way ANOVA, the Kruskal–Wallis test, and Fisher's post hoc test. Follicle autophagy staining in granulosa cell layers (mean intensity ± SEM) in the general follicle population (C) and in primordial follicles on day 3 (D) evaluated by using one-way ANOVA and Fisher's post hoc test. p value references: *$p < 0.05$

Follicle autophagy

A total of 966 follicles were evaluated for the LC3B marker: 198 in non-grafted controls, respectively 220 and 200 in the 2-step/ASCs+OT and OT groups on day 3, and respectively 198 and 150 in the 2-step/ASCs+OT and OT groups on day 10. The global staining index of the LC3B marker was similar in all groups over time compared to non-grafted controls (Fig. 3c). When examining each follicle stage individually, however, lower values were detected in small primordial follicles in the OT group 3 days after transplantation than in non-grafted controls, while no difference was found between the 2-step/ASCs+OT group and non-grafted controls ($p = 0.03$) (Fig. 3d).

PI3K/Akt pathway activation

A total of 174 primordial follicles were investigated for the FOXO1 marker: 79 in non-grafted controls, respectively 35 and 28 in the 2-step/ASCs+OT and OT groups on day 3, and respectively 17 and 15 in the 2-step/ASCs+OT and OT groups on day 10 (Fig. 4A, B). With respect to small primordial follicles, a significant nucleus-to-cytoplasm shift was detected in the OT group 3 days (ratio measures ± SD: 0.9 ± 0.2, $p = 0.01$) and 10 days (1.2 ± 0.05, $p = 0.03$) after transplantation compared to non-grafted controls (2.34 ± 1.03). No difference was found between the 2-step/ASCs+OT group and non-grafted controls at any time point (day 3: 1.86 ± 0.6; day 10: 2 ± 0.45). In terms of intermediate follicles, no difference was observed between any groups or time points (Fig. 4C).

Hippo pathway disruption

A total of 271 primordial follicles were assessed for the YAP marker: 91 in non-grafted controls, respectively 43 and 50 in the 2-step/ASCs+OT and OT groups on day 3, and 47 and 40 in the 2-step/ASCs+OT and OT groups on day 10 (Fig. 5A). One hundred twenty-two growing follicles were also analyzed for the YAP marker: 19 in non-grafted controls, respectively 27 and 27 in the 2-step/ASCs+OT and OT groups on day 3, and respectively 26 and 23 in the 2-step/ASCs+OT and OT groups on day 10 (Fig. 5B). Analysis of the subcellular localization of YAP evidenced nuclear retention in small primordial and intermediate follicles. No significant difference in ratio measures was found between non-grafted controls and grafted groups on days 3 or 10 post-transplantation. Considering growing follicles, nuclear YAP localization was predominantly observed in non-grafted controls. In the grafted groups, significantly lower values were obtained in the 2-step/ASCs+OT group compared to the OT group (0.9 ± 0.04 vs 1.2 ± 0.2, $p = 0.008$) after 3 days of grafting. Similarly, nuclear YAP localization substantially decreased in the OT group over time (from day 3 to day 10) (1.2 ± 0.2 vs 1 ± 0.03, $p = 0.04$) (Fig. 5C).

Discussion

While ovarian tissue transplantation is an effective strategy for fertility restoration, the avascular nature of the grafting technique itself induces major stress in transplanted tissue, with significant loss of the follicle reserve, which somewhat limits its effectiveness [6, 7]. Preparation of the transplantation site with ASCs is able to shorten the hypoxic period and consequently reduce follicle loss after grafting. Indeed, the number of follicles was significantly higher 7 days after transplantation with this strategy, together with a significant drop in follicle death rates and growing follicle proportions [19, 28]. Moreover, the primordial follicle pool was found to be better

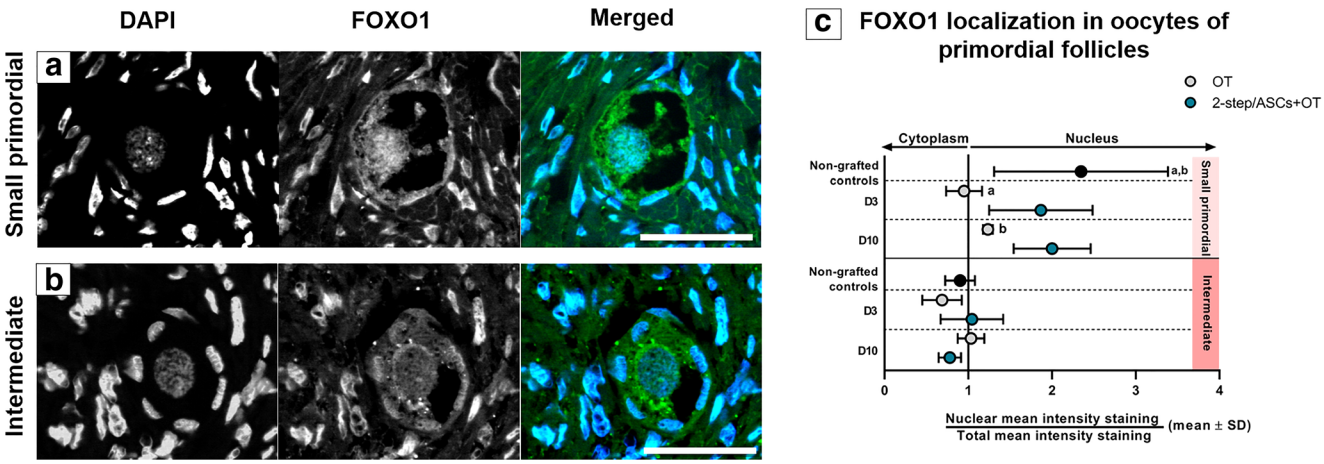


Fig. 4 FOXO1 localization. Immunofluorescence targeting FOXO1 (green color) and subcellular localization of primordial follicles in oocytes. Nuclear localization (A) in non-activated small primordial follicles; cytoplasmic localization (B) in activated intermediate follicles. FOXO1 localization analysis (nuclear mean intensity staining/total mean intensity staining ± SD) in small primordial and intermediate follicles evaluated by using one-way ANOVA and Fisher's post hoc test. Statistical significance was expressed using different letters ($p < 0.05$). Scale bar: 20 μm

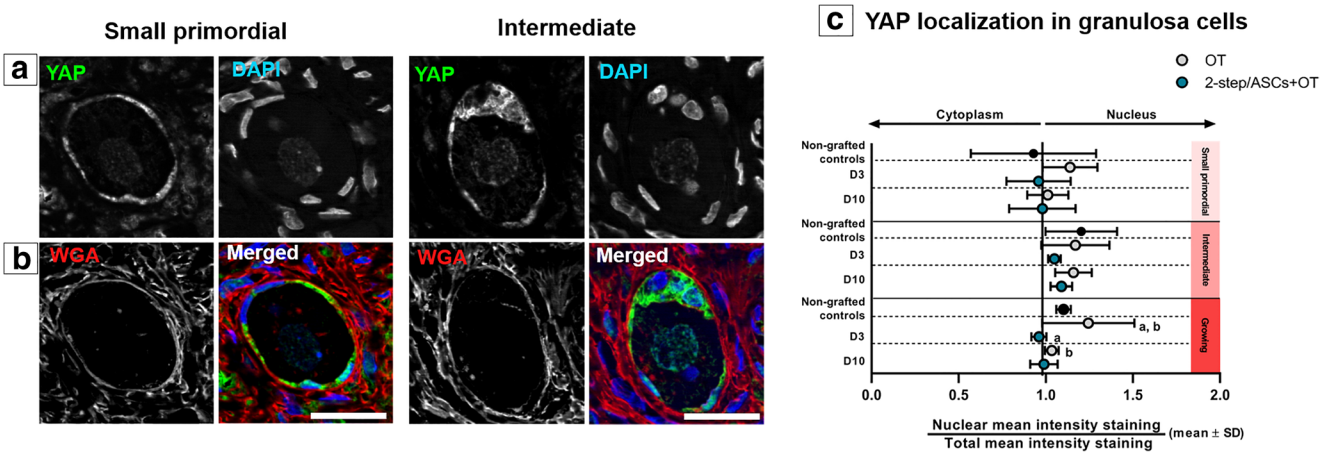


Fig. 5 YAP localization. Immunofluorescence targeting YAP (green color) and subcellular localization analysis in granulosa cells delimited by plasmatic membrane counterstaining (red color). Nuclear and cytoplasmic localizations (A) in small primordial (B) and intermediate follicles (C). YAP localization analysis (nuclear mean intensity staining/total mean intensity staining ± SD) in small primordial, intermediate, and growing follicles evaluated by using one-way ANOVA, the Kruskal–Wallis test, and Fisher's post hoc test. Statistical significance is expressed using different letters ($p < 0.05$). Scale bar: 20 μm

preserved after 6 months of grafting with ASCs, showing similar endocrine function resumption to the standard transplantation procedure [29]. In the present study, we were able to prove that ASCs have a positive impact on grafted tissue by significantly reducing follicle loss both 3 and 10 days after grafting. They are also crucial to protecting the primordial follicle pool by modulation of both follicle death and activation mechanisms.

The primordial follicle pool

In this study, we set out to investigate follicle density, with particular scruting of primordial follicle pool. For this purpose, we applied Gougeon et al.'s classification, which considers the primordial follicle reserve to be made up of two different subpopulations: primordial follicles in a quiescent state and intermediate follicles that have already started transformation of their granulosa cells from flattened to cuboidal [24, 26]. Preservation of the primordial follicle pool over and above all other follicle stages is of key importance for transplantation of ovarian tissue. The size and quality of the primordial follicle reserve are indeed major determinants, not only of graft lifespan but also of fertility potential after grafting. The primordial follicle pool constitutes the long-term stockpile of the ovary, whose maintenance depends on a balance between quiescence and the growth to the antral follicle stage for possible selection [24, 30]. Primordial follicles pass through an intermediate stage before reaching primary status. A dynamic balance exists between these two states, as intermediate follicles are more prone to further growth, but they also appear to be able to return to quiescence in small proportions [24, 26].

The destiny of primordial follicles during a stressful event is still contentious. Indeed, there are two main mechanisms proposed in the literature to explain the rapid follicle depletion seen after transplantation. One is direct follicle death as a consequence of hypoxia/ischemia, through activation of either apoptosis or necrosis [10]. The other is massive primordial follicle activation occurring as a result of numerous potential triggers of signaling pathways involved in follicle activation and growth [9, 12, 14]. Our findings revealed a massive drop in small primordial follicles after standard transplantation, while this follicle population appeared to be maintained with use of ASCs. Regarding growing follicles, including the intermediate stage, no upturn was observed after 3 or 10 days in any of the groups. These results may shift the balance in favor of follicle death as the major cause of hypoxia-related primordial follicle pool depletion, as we failed to detect any increase in growing follicles.

Follicle death

To address the hypothesis of follicle death as the major cause of loss, we investigated proportions of atretic follicles between different groups over time. Follicle atresia is the resulting feature of several death processes [31]. It occurs physiologically in ovarian tissue together with follicle selection, but it also represents the final outcome after necrosis, apoptosis, and non-apoptotic cell death processes.

In our findings, a significant increase was observed in atretic follicles in the OT group, but there was no significant increase in atretic follicle proportions when ASCs were used, pointing to their role in preventing large-scale follicle loss by decreasing cell death [8]. Consistent with our histological findings, analysis of c-caspase-3-positive follicles showed increased apoptotic follicle proportions soon after transplantation using the standard grafting procedure compared to 2-step transplantation with ASCs. These findings support the hypothesis that ASCs reduce follicle loss by decreasing

hypoxia/ischemia-related follicle death. However, their antiapoptotic impact could either be due to shortened hypoxia or be a direct consequence of the stem cell secretome that was shown to exert such an effect in other models [32, 33].

Follicle autophagy

Evaluation of follicle behavior under hypoxia-related stress led us to investigate another crucial process for cell adaptation to stress and survival. Autophagy is a protective process of self-degradation in order to ensure cell survival and promote cell renewal in stressful conditions [34]. Indeed, tissue starvation, hypoxia, or oxidative stress can result in accumulation of undigested materials. Depending on a cell's inability to resist prolonged or severe stress, subsequent cell death may or may not occur [35, 36]. Under physiological conditions, autophagy plays a role in maintaining primordial follicle quiescence of the ovary [37]. In fact, accelerated depletion of the primordial follicle pool was observed in studies using knockout animal models for autophagy-related genes [38], and genetic mutations related to autophagy impairment were observed in patients suffering premature ovarian insufficiency [39].

Mature autophagosomes, expressing the LC3B marker, can be found in granulosa cells at all follicle stages throughout the whole post-transplantation period. This is not surprising, since the process of preservation of ovarian cortex is a stressful event, and enhancement of cell protection effectors may be activated early as preconditioning mechanisms for further tissue survival [40]. Conversely, we did not expect to observe lower autophagic activity in primordial follicles so soon after transplantation using the one-step procedure. These findings suggest loss of cell mechanisms that maintain primordial follicle quiescence in favor of the hypothesis of increased activation. Corroborating this hypothesis, PI3K/Akt is able to inhibit autophagy in severe hypoxic conditions through mTORC1, in order to create a balance towards anabolic activity for cell growth over catabolism of proteins [41, 42].

Follicle activation

Increased primordial follicle activation observed soon after ovarian tissue transplantation has been associated with activation of the PI3K/Akt pathway [14, 43]. Maintenance of the quiescent state appears to be related to FOXO1–3 activity, whose cytoplasmic shift is related to the start of cross-talk between the oocyte and granulosa cells before effective follicle growth, namely transformation from flattened to cuboidal granulosa cells [29]. Indeed, its constitutive presence or absence in specific knockout animal models was found to be responsible for primordial follicle recruitment, but not further follicle growth [44, 45]. For these reasons, we analyzed small primordial and intermediate follicles separately. As expected, activation of the PI3K/Akt pathway was observed in oocytes of intermediate follicles irrespective of transplantation, confirming that activation of this signaling pathway occurs before morphological changes to granulosa cells.

On the other hand, no significant FOXO1 nuclear trafficking was observed in small primordial follicles before transplantation, confirming their quiescent state. After transplantation, a significant increase was detected in PI3K/Akt pathway activation with the standard procedure, confirming that early primordial follicle activation, triggered by this signaling pathway for cell survival and proliferation, plays a role in depletion of the primordial follicle pool soon after grafting [14, 43].

Small primordial follicles appeared to be undisturbed by ASCs. These results indicate that follicle activation can be mitigated by decreasing hypoxia early after transplantation. Indeed, interaction between the PI3K/Akt pathway and hypoxia-related cellular responses is already known, as a number of growth factors released in hypoxic conditions, like VEGF, may trigger Akt phosphorylation [46, 47]. Using ASCs, we were able to prove that shortening the hypoxic period prevents massive follicle loss. The mechanisms by which ASCs affect the PI3K/Akt pathway may either be associated with the hypoxia-related response or be directly triggered by their presence in the transplantation site. We believe that further experiments, probably involving development of an in vitro model, should be carried out to investigate the effect of the ASC secretome, including VEGF, on primordial follicle behavior.

We also decided to investigate another signaling pathway in order to evaluate whether ASCs impact follicle growth. The Hippo pathway plays a major role in promoting follicle growth, rather than initiating follicle activation in primordial follicles [12, 13]. Analysis of YAP nuclear translocation in the present study confirmed this assertion, as no significant difference was detected in small primordial and intermediate follicles after grafting, irrespective of transplantation technique. These findings confirm that manipulation of the ovarian cortex for cryopreservation is sufficient to impact this signaling pathway, as observed in other studies [13, 48]. Ovarian cortex fragmentation actually facilitates conversion of globular actin (G-actin) into filamentous actin (F-actin), inducing disruption of Hippo signaling [49]. However, greater pathway disruption was identified in growing follicles of fragments grafted with the standard procedure.

When contemplating the ASC group, data suggest that these cells can repress the Hippo pathway, as seen in growing follicles soon after transplantation. This is consistent with the hypothesis that grafting ASCs does indeed shorten the hypoxic period, thereby impacting the pace of follicle growth too.

Limitations of the study

Although this study was able to demonstrate an impact of ASCs on both primordial follicle death and activation soon

after transplantation, it did not investigate interactions between these two biological events, which may well be interconnected. Indeed, the response to tissue stress may be oriented towards either cell death or cell survival, depending on numerous factors involved in the event itself. Further studies are needed to elucidate the interplay between these processes and their modulation in hypoxic and normoxic conditions in transplanted ovarian tissue.

Conclusions

Two-step transplantation using ASCs has proved its effectiveness in addressing the issue of massive follicle loss due to post-transplantation hypoxia. ASCs exert a degree of protection, especially on primordial follicles, by means of major mechanisms, namely direct diminution of follicle death (necrosis and apoptosis) and negative modulation of the signaling pathways (PI3K/Akt and Hippo) involved in follicle activation and growth. These data confirm that both follicle death and abnormal activation mechanisms play a role in follicle depletion soon after ovarian tissue damage. They also prove that reduction of hypoxia by preparation of the grafting site with ASCs is able to counteract them, and hence significantly improve follicle outcomes after transplantation.

Supplementary Information The online version contains supplementary material available at https://doi.org/10.1007/s10815-020-02005-z.

Funding This study was supported by grants from the Fonds National de la Recherche Scientifique de Belgique (F.R.S.-FNRS/FRIA FC29657 awarded to Luciana Cacciottola, FNRS-PDR Convention T.0077.14, the Excellence of Science FNRS–EOS number 30443682, and grant 5/4/150/5 awarded to Marie-Madeleine Dolmans), Fonds Spéciaux de Recherche, Fondation St Luc and the Foundation Against Cancer, and donations from the Ferrero family.

Compliance with ethical standards

Conflict of interest The authors declare that they have no conflict interest.

References

1. Dolmans MM, Lambertini M, Macklon KT, Almeida Santos T, Ruiz-Casado A, Borini A, et al. EUropean REcommendations for female FERtility preservation (EU-REFER): a joint collaboration between oncologists and fertility specialists. Crit Rev Oncol Hematol. 2019;138:233–40. https://doi.org/10.1016/j.critrevonc.2019.03.010.
2. Donnez J, Dolmans MM. Fertility preservation in women. N Engl J Med. 2017;377(17):1657–65. https://doi.org/10.1056/NEJMra1614676.
3. Dolmans MM, Falcone T, Patrizio P. Importance of patient selection to analyze in vitro fertilization outcome with transplanted cryopreserved ovarian tissue. Fertil Steril. 2020;114:279–80 in press.
4. Dolmans MM, Manavella DD. Recent advances in fertility preservation. J Obstet Gynaecol Res. 2019;45(2):266–79. https://doi.org/10.1111/jog.13818.
5. Van Eyck AS, Jordan BF, Gallez B, Heilier JF, Van Langendonckt A, Donnez J. Electron paramagnetic resonance as a tool to evaluate human ovarian tissue reoxygenation after xenografting. Fertil Steril. 2009;92(1):374–81. https://doi.org/10.1016/j.fertnstert.2008.05.012.
6. Cacciottola L, Manavella DD, Amorim CA, Donnez J, Dolmans MM. In vivo characterization of metabolic activity and oxidative stress in grafted human ovarian tissue using microdialysis. Fertil Steril. 2018;110(3):534–544.e3. https://doi.org/10.1016/j.fertnstert.2018.04.009.
7. Nisolle M, Casanas-Roux F, Qu J, Motta P, Donnez J. Histologic and ultrastructural evaluation of fresh and frozen-thawed human ovarian xenografts in nude mice. Fertil Steril. 2000;74(1):122–9. https://doi.org/10.1016/s0015-0282(00)00548-3.
8. Spears N, Lopes F, Stefansdottir A, Rossi V, De Felici M, Anderson RA, et al. Ovarian damage from chemotherapy and current approaches to its protection. Hum Reprod Update. 2019;25(6):673–93. https://doi.org/10.1093/humupd/dmz027.
9. Kalich-Philosoph L, Roness H, Carmely A, Fisher-Bartal M, Ligumski H, Paglin S, et al. Cyclophosphamide triggers follicle activation and "burnout"; AS101 prevents follicle loss and preserves fertility. Sci Transl Med. 2013;5(185):185ra62. https://doi.org/10.1126/scitranslmed.3005402.
10. Luan Y, Edmonds ME, Woodruff TK, Kim SY. Inhibitors of apoptosis protect the ovarian reserve from cyclophosphamide. J Endocrinol. 2019;240(2):243–56. https://doi.org/10.1530/JOE-18-0370.
11. Zhang H, Liu K. Cellular and molecular regulation of the activation of mammalian primordial follicles: somatic cells initiate activation in adulthood. Hum Reprod Update. 2015;21(6):779–86. https://doi.org/10.1093/humupd/dmv037.
12. Kawamura K, Cheng Y, Suzuki N, Deguchi M, Sato Y, Takae S, et al. Hippo signaling disruption and Akt stimulation of ovarian follicles for infertility treatment. Proc Natl Acad Sci U S A. 2013;110(43):17474–9. https://doi.org/10.1073/pnas.1312830110.
13. Grosbois J, Demeestere I. Dynamics of PI3K and Hippo signaling pathways during in vitro human follicle activation. Hum Reprod. 2018;33(9):1705–14. https://doi.org/10.1093/humrep/dey250.
14. Masciangelo R, Hossay C, Donnez J, Dolmans MM. Does the Akt pathway play a role in follicle activation after grafting of human ovarian tissue? Reprod BioMed Online. 2019;39(2):196–8. https://doi.org/10.1016/j.rbmo.2019.04.007.
15. Gavish Z, Spector I, Peer G, Schlatt S, Wistuba J, Roness H, et al. Follicle activation is a significant and immediate cause of follicle loss after ovarian tissue transplantation. J Assist Reprod Genet. 2018;35(1):61–9. https://doi.org/10.1007/s10815-017-1079-z.
16. Zhang Z, Yao L, Yang J, Wang Z, Du G. PI3K/Akt and HIF-1 signaling pathway in hypoxia-ischemia (Review). Mol Med Rep. 2018;18(4):3547–54. https://doi.org/10.3892/mmr.2018.9375.
17. Xie Y, Shi X, Sheng K, Han G, Li W, Zhao Q, et al. PI3K/Akt signaling transduction pathway, erythropoiesis and glycolysis in hypoxia (Review). Mol Med Rep. 2019;19(2):783–91. https://doi.org/10.3892/mmr.2018.9713.
18. Manavella DD, Cacciottola L, Desmet CM, Jordan BF, Donnez J, Amorim CA, et al. Adipose tissue-derived stem cells in a fibrin implant enhance neovascularization in a peritoneal grafting site: a potential way to improve ovarian tissue transplantation. Hum Reprod. 2018;33(2):270–9. https://doi.org/10.1093/humrep/dex374.
19. Manavella DD, Cacciottola L, Pommé S, Desmet CM, Jordan BF, Donnez J, et al. Two-step transplantation with adipose tissue-derived stem cells increases follicle survival by enhancing vascularization in xenografted frozen-thawed human ovarian tissue. Hum

Reprod. 2018;33(6):1107–16. https://doi.org/10.1093/humrep/dey080.
20. Manavella DD, Cacciottola L, Payen VL, Amorim CA, Donnez J, Dolmans MM. Adipose tissue-derived stem cells boost vascularization in grafted ovarian tissue by growth factor secretion and differentiation into endothelial cell lineages. Mol Hum Reprod. 2019;25(4):184–93. https://doi.org/10.1093/molehr/gaz008.
21. Dolmans MM, Jadoul P, Gilliaux S, Amorim CA, Luyckx V, Squifflet J, et al. A review of 15 years of ovarian tissue bank activities. J Assist Reprod Genet. 2013;30(3):305–14. https://doi.org/10.1007/s10815-013-9952-x.
22. Chiti MC, Dolmans MM, Donnez J, Amorim CA. Fibrin in reproductive tissue engineering: a review on its application as a biomaterial for fertility preservation. Ann Biomed Eng. 2017;45(7):1650–63. https://doi.org/10.1007/s10439-017-1817-5.
23. Dath C, Van Eyck AS, Dolmans MM, Romeu L, Delle Vigne L, Donnez J, et al. Xenotransplantation of human ovarian tissue to nude mice: comparison between four grafting sites. Hum Reprod. 2010;25(7):1734–43. https://doi.org/10.1093/humrep/deq131.
24. Gougeon A, Chainy G. Morphometric studies of small follicles in ovaries of women at different ages. J Reprod Fertil. 1987;81(2):433–42. https://doi.org/10.1530/jrf.0.0810433.
25. Anderson RA, McLaughling M, Wallace WH, Albertini DF, Telfer EE. The immature human ovary shows loss of abnormal follicles and increasing follicle development competence through childhood and adolescence. Hum Reprod. 2014;29(1):97–106. https://doi.org/10.1093/humrep/det388.
26. Gougeon A, Busso D. Morphologic and functional determinants of primordial and primary follicles in the monkey ovary. Mol Cell Endocrinol. 2000;163(1–2):33–42. https://doi.org/10.1016/s0303-7207(00)00220-3.
27. Amorim CA, Donnez J, Dehoux JP, Scalercio SR, Squifflet J, Dolmans MM. Long-term follow-up of vitrified and autografted baboon (Papio anubis) ovarian tissue. Hum Reprod. 2019;34(2):323–34.
28. Dolmans MM, Cacciottola L, Amorim CA, Manavella D. Translational research aiming to improve survival of ovarian tissue transplants using adipose tissue-derived stem cells. Acta Obstet Gynecol Scand. 2019;98(5):665–71. https://doi.org/10.1111/aogs.13610.
29. Cacciottola L, Nguyen TYT, Chiti MC, Camboni A, Amorim CA, Donnez J, et al. Long-term advantages of ovarian reserve maintenance and follicle development using adipose tissue-derived stem cells in ovarian tissue transplantation. J Clin Med. 2020;9(9):E2980. https://doi.org/10.3390/jcm9092980.
30. Picton HM, Harris SE, Muruvi W, Chambers EL. The in vitro growth and maturation of follicles. Reproduction. 2008;136(6):703–15. https://doi.org/10.1530/REP-08-0290.
31. Hirshfield AN. Development of follicles in the mammalian ovary. Int Rev Cytol. 1991;124:43–101. https://doi.org/10.1016/s0074-7696(08)61524-7.
32. Bonafede R, Brandi J, Manfredi M, Scambi I, Schiaffino L, Merigo F, et al. The anti-apoptotic effect of ASC-exosomes in an in vitro ALS model and their proteomic analysis. Cells. 2019;8(9):1087. https://doi.org/10.3390/cells8091087.
33. Shih YC, Lee PY, Cheng H, Tsai CH, Ma H, Tarng DC. Adipose-derived stem cells exhibit antioxidative and antiapoptotic properties to rescue ischemic acute kidney injury in rats. Plast Reconstr Surg. 2013;132(6):940e–51e. https://doi.org/10.1097/PRS.0b013e3182a806ce.
34. Ravanan P, Srikumar IF, Talwar P. Autophagy: the spotlight for cellular stress responses. Life Sci. 2017;188:53–67. https://doi.org/10.1016/j.lfs.2017.08.029.
35. Mizushima N, Yamamoto A, Matsui M, Yoshimori T, Oshumu Y. In vivo analysis of autophagy in response to nutrient starvation using transgenic mice expressing a fluorescent autophagosome marker. Mol Biol Cell. 2004;15(3):1101–11. https://doi.org/10.1091/mbc.e03-09-0704.
36. Yadav AK, Yadav PK, Chaudhary GR, Tiwari M, Gupta A, Sharma A, et al. Autophagy in hypoxic ovary. Cell Mol Life Sci. 2019;76(17):3311–22. https://doi.org/10.1007/s00018-019-03122-4.
37. Gawriluk TR, Hale AN, Flaws JA, Dillon CP, Green DR, Rucker EB 3rd. Autophagy is a cell survival program for female germ cells in the murine ovary. Reproduction. 2011;141(6):759–65. https://doi.org/10.1530/REP-10-0489.
38. Song ZH, Yu HY, Wang P, Mao GK, Liu WX, Li MN, et al. Germ cell-specific Atg7 knockout results in primary ovarian insufficiency in female mice. Cell Death Dis. 2015;6(1):e1589. Published 2015 Jan 15. https://doi.org/10.1038/cddis.2014.559.
39. Delcour C, Amazit L, Patino LC, Magning F, Fagart J, Delemer B, et al. ATG7 and ATG9A loss-of-function variants trigger autophagy impairment and ovarian failure. Genet Med. 2019;21(4):930–8. https://doi.org/10.1038/s41436-018-0287-y.
40. Carden DL, Granger DN. Pathophysiology of ischaemia-reperfusion injury. J Pathol. 2000;190(3):255–66. https://doi.org/10.1002/(SICI)1096-9896(200002)190:3<255::AID-PATH526>3.0.CO;2-6.
41. Sciarretta S, Volpe M, Sadoshima J. Mammalian target of rapamycin signaling in cardiac physiology and disease. Circ Res. 2014;114(3):549–64. https://doi.org/10.1161/CIRCRESAHA.114.302022.
42. Neufeld TP. TOR-dependent control in autophagy: biting the hand that feeds. Curr Opin Cell Biol. 2010;22(2):157–68. https://doi.org/10.1016/j.ceb.2009.11.005.
43. Masciangelo R, Hossay C, Chiti MC, Manavella DD, Amorim CA, Donnez J, et al. Role of the PI3K and Hippo pathways in follicle activation after grafting of human ovarian tissue. J Assist Reprod Genet. 2020;37(1):101–8. https://doi.org/10.1007/s10815-019-01628-1.
44. Castrillon DH, Miao L, Kollipara R, Hroner JW, De Pinho RA. Suppression of ovarian follicle activation in mice by transcription factor Foxo3a. Science. 2003;301(5630):215–8. https://doi.org/10.1126/science.1086336.
45. Liu L, Rajareddy S, Reddy P, Du C, Jagarlamudi K, Shen Y, et al. Infertility caused by retardation of follicular development in mice with oocyte-specific expression of Foxo3a. Development. 2007;134(1):199–209. https://doi.org/10.1242/dev.02667.
46. Ma X, Bai Y. IGF-1 activates the PI3K/Akt signaling pathway via upregulation of secretory clusterin. Mol Med Rep. 2012;6(6):1433–7. https://doi.org/10.3892/mmr.2012.1110.
47. Dudu V, Able RA Jr, Rotari V, Kong Q, Vazquez M. Role of epidermal growth factor-triggered PI3K/Akt signaling in the migration of medulloblastoma-derived cells. Cell Mol Bioeng. 2012;5(4):502–413. https://doi.org/10.1007/s12195-012-0253-8.
48. Dolmans MM, Cordier F, Amorim CA, Donnez J, Vander Linden C. In vitro activation prior to transplantation of human ovarian tissue: is it truly effective? Front Endocrinol (Lausanne). 2019;10:520. Published 2019 Aug 2. https://doi.org/10.3389/fendo.2019.00520.
49. Devos M, Groisbois J, Demeestere I. Interaction between PI3K/AKT and Hippo pathways during in vitro follicular activation and response to fragmentation and chemotherapy exposure using a mouse immature ovary model. Biol Reprod. 2020;102(3):717–29. https://doi.org/10.1093/biolre/ioz215.

Publisher's note Springer Nature remains neutral with regard to jurisdictional claims in published maps and institutional affiliations.